J Mater Sci: Mater Electron (2016) 27:11293–11298
DOI 10.1007/s10854-016-5252-4

Microwave dielectric properties of low-fired $CoNb_2O_6$ ceramics with B_2O_3 addition

Yun Zhang[1] · Shuya Liu[1] · Yingchun Zhang[1] · Maoqiao Xiang[1]

Received: 14 April 2016 / Accepted: 23 June 2016 / Published online: 29 June 2016

Abstract Low-fired B_2O_3-doped $CoNb_2O_6$ microwave dielectric ceramics were synthesized via conventional solid-state method. The effects of B_2O_3 additives on their sintering behavior, phase composition, and microwave dielectric properties were investigated systematically. The addition of B_2O_3 as liquid phase successfully lowered the sintering temperature of $CoNb_2O_6$ ceramics from 1200 to 1000 °C. The system remained orthorhombic columbite phase at the level of 0.5–1.5 wt% B_2O_3 addition. However, a trace amount of $Co_4Nb_2O_9$ second phase with major $CoNb_2O_6$ phase was observed for the 2 wt% B_2O_3-added sample. The microwave dielectric properties were found to strongly correlate with the sintering temperature as well as the amount of B_2O_3 addition. With 1.5 wt% B_2O_3, $CoNb_2O_6$ ceramics sintered at 1000 °C possessed optimum microwave dielectric properties with an ε_r of 22.4, a high $Q \times f$ of 43,979 GHz, and a τ_f of −46.2 ppm/°C.

1 Introduction

With the rapid development of wireless communication industry, low-temperature cofired ceramic (LTCC) technology has been extensively investigated for miniaturization and integration of components [1, 2]. In LTCC devices fabrication, the ceramics are co-fired with highly conductive electrode materials, such as silver (melting point 961 °C) and copper (melting point 1083 °C), to form three-dimensional modules [3]. Therefore, the ceramics are required to have low sintering temperature which can be co-sinterable with the metal electrodes. In addition, high relative permittivity ($\varepsilon_r > 20$, to allow miniaturization of the component), low dielectric losses ($Q > 5000$, where $Q = 1/\tan\delta$, to improve selectivity at microwave frequencies), and a near zero temperature coefficient of resonant frequency ($\tau_f \sim 0$ ppm/°C, for temperature stability) are also the key characteristics for practical applications [4, 5]. The optimal balance of these properties is one of the major challenges faced by electronic industry.

The binary ceramic with general formula MNb_2O_6 (M^{2+} = Mg, Ca, Mn, Co, Ni, Zn) was a potential candidate for mechanical filter coatings and electrical applications [6]. Among the niobates investigated, of particular interest was $CoNb_2O_6$. As to its dielectric properties, the data reported in the literatures were contradictory. According to Lee et al. [7], $CoNb_2O_6$ had a rather low electrical Q ($Q \times f = 11{,}300$ GHz), whereas Pullar [8] achieved notably higher Q value: $Q \times f = 41{,}700$ GHz. Recently, Belous [9] reported its $Q \times f$ as high as 82,000 GHz. However, the $CoNb_2O_6$ ceramics possessed high sintering temperature (>1150 °C) in nearly all cases. As a result, liquid phase flux such as CeO_2, WO_3, V_2O_5 and CuO were introduced to reduce the sintering temperature [10]. Unfortunately, CeO_2 and WO_3 had negative effect on the densification of the niobate. Additions of both V_2O_5 and CuO resulted in $Q \times f$ under half that of the pure columbite. So it is of great significance if we can decrease the sintering temperature with desired properties. Considering its low melting point, B_2O_3 was usually selected as an effective sintering aid to develop low-fired dielectric ceramics. For instance, B_2O_3 addition to Zn_2SiO_4 ceramics significantly reduced the sintering temperature to 900 °C without deterioration of the dielectric properties [11].

✉ Yingchun Zhang
zycustb@163.com

[1] School of Materials Science and Engineering, University of Science and Technology Beijing, Beijing 100083, People's Republic of China

Besides, Lv and Zuo [12] found the microwave dielectric characteristics of 3 wt% B_2O_3-doped $0.5Ba_3(VO_4)_2$−$0.5Zn_{1.87}SiO_{3.87}$ ceramics sintered at 925 °C to be $\varepsilon_r = 10$, $Q \times f = 40{,}800$ GHz, and $\tau_f = 0.5$ ppm/°C. Thus, B_2O_3 was employed to lower the sintering temperature of $CoNb_2O_6$ ceramics in the present work. Furthermore, the influence of B_2O_3 additions on their sintering behavior, phase composition and microwave dielectric properties was investigated systematically.

2 Experimental procedures

$CoNb_2O_6$ ceramics were synthesized by conventional solid state reaction route. High-purity oxide powders (>99.9 %) of CoO, Nb_2O_5 and B_2O_3 were adopted as raw chemicals. Stoichiometric amounts of CoO and Nb_2O_5 were mixed with ethanol in polyethylene bottles. Subsequently, the slurries were dried, screened by a 200-mesh sieve, and calcined at 1000 °C for 4 h to obtain $CoNb_2O_6$. Different weight percentages of B_2O_3 were then added to the calcined powders. After remilling and sieving, the resultant powders with organic binder (5 wt% polyvinyl alcohol) were uniaxially compacted into cylinders of 10 mm in diameter and 6 mm in thickness at a pressure of 150 MPa. Finally, the green bodies were sintered in the temperature range of 900–1300 °C for 4 h. During sintering, both the heating rate and cooling rate were maintained at 3 °C/min.

The relative densities of sintered samples were identified by the common Archimedes method. Crystal structure was undertaken by X-ray diffraction (XRD, Rigaku, DMAX-RB, Japan) with Cu $K\alpha$ radiation. The microstructure was characterized by scanning electron microscopy (SEM; JSM-6480LV) coupled with EDS spectroscopy. The microwave dielectric properties were evaluated by a network analyzer (HP8720ES, Hewlett-Packard, Santa, Rosa, CA). The dielectric constant was measured according to the Hakki–Coleman post-resonator method [13] by exciting the TE_{011} resonant mode of the DR using the electric probe of an antenna as suggested by Courtney [14]. The unloaded quality factors were measured using the $TE_{01\delta}$ mode in the cavity method [15]. All measurements were made in the frequency range of 4–9 GHz at room temperature. Temperature coefficients of the resonant frequencies of the TE_{011} mode were obtained in the temperature range from 25 to 80 °C. The τ_f values were defined by the following relationship:

$$\tau_f = \frac{f_2 - f_1}{f_1(T_2 - T_1)} \quad (1)$$

where f_1 and f_2 were the resonant frequency at T_1 and T_2, respectively.

3 Results and discussions

The relative densities of B_2O_3-doped $CoNb_2O_6$ ceramics sintered at various sintering temperatures are offered in Fig. 1. Pure $CoNb_2O_6$ ceramic was well sintered to approach 95.29 % theoretical density only when the sintering temperature was raised to 1200 °C. When a small amount of B_2O_3 was added, the relative density reached its saturated value at around 1100 °C. But in the case of >1.0 wt% added B_2O_3, the sintering behavior was promoted remarkably. A maximum relative density of about 96.72 % was obtained for the specimen with 1.5 wt% B_2O_3 sintered at 1000 °C. The possible reason for the enhanced

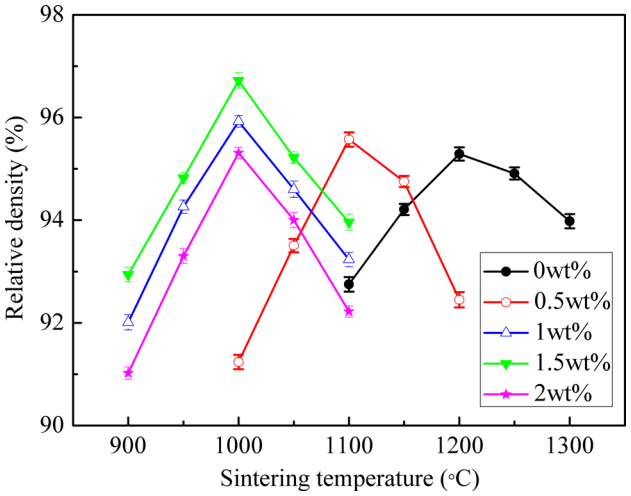

Fig. 1 Relative densities of $CoNb_2O_6$ ceramics with different B_2O_3 additions as a function of sintering temperature

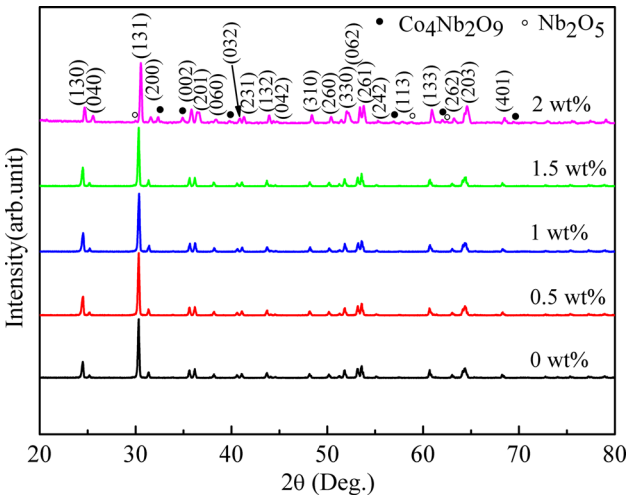

Fig. 2 XRD patterns of $CoNb_2O_6$ ceramics added with various amounts of B_2O_3 additions **a** pure $CoNb_2O_6$ ceramic, at 1200 °C, **b** 0.5 wt%, at 1100 °C, **c** 1 wt%, at 1000 °C, **d** 1.5 wt%, at 1000 °C, **e** 2 wt%, at 1000 °C

sinterability might come from the presence of liquid phase during sintering, since the melting point of B_2O_3 was just 450 °C [16, 17]. In the presence of a liquid phase, particle rearrangement became easier and mass transport by grain-boundary diffusion took place much faster, leading to enhanced densification kinetics. However, further addition of the flux resulted in an apparent decrease in densification.

Figure 2 presents the XRD patterns of $CoNb_2O_6$ ceramics with different B_2O_3 additions. It revealed that single $CoNb_2O_6$ phase (JCPDS NO. 32-0304) was obtained for the B_2O_3-free sample. Similar XRD patterns were detected at the level of 0.5–1.5 wt% B_2O_3 addition. However, when the B_2O_3 content was increased up to 2 wt%, a trace amount of $Co_4Nb_2O_9$ (JCPDS NO. 38-1457) and Nb_2O_5 (JCPDS NO.26-0885) secondary phases were formed along with the major $CoNb_2O_6$ phase. The preparation process and sintering condition were all the same for the 1–2 wt% B_2O_3-added samples. Based on this, it might be concluded that high concentration of B_2O_3 favored the phase transformation from $CoNb_2O_6$ to $Co_4Nb_2O_9$. To be noted that this transformation was partial, because the amount of second phases was rather small. Columbite $CoNb_2O_6$ had been reported to crystallize in an orthorhombic α-PbO_2-type structure [18]. Whereas for $Co_4Nb_2O_9$, it performed hexagonal corundum structure with space group P-3c1 [19]. But in fact both of them were the combination of CoO6 and NbO6 octahedra. A higher B_2O_3 doping level might influence the Nb:Co ratio in the unit cell and, hence the crystallographic distortion. So $Co_4Nb_2O_9$ was formed through the reaction shown below. Systematic analysis is still needed to verify this explanation.

$$4CoNb_2O_6 \rightarrow Co_4Nb_2O_9 + 3Nb_2O_5 \quad (2)$$

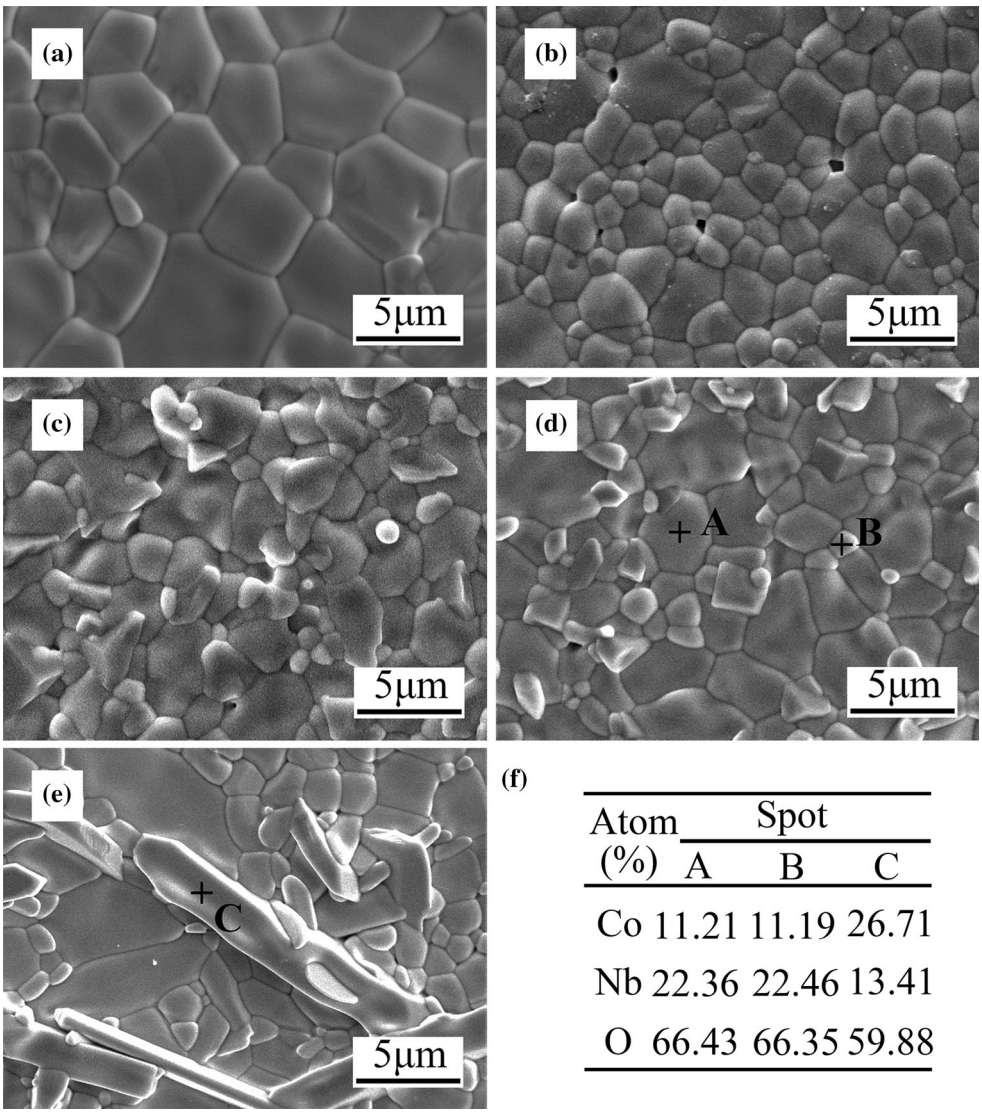

(f)

Atom (%)	Spot A	Spot B	Spot C
Co	11.21	11.19	26.71
Nb	22.36	22.46	13.41
O	66.43	66.35	59.88

Fig. 3 Scanning electron micrographs of $CoNb_2O_6$ ceramics with B_2O_3 additions: **a** pure $CoNb_2O_6$ ceramic, at 1200 °C, **b** 0.5 wt%, at 1100 °C, **c** 1 wt%, at 1000 °C, **d** 1.5 wt%, at 1000 °C, **e** 2 wt%, at 1000 °C, and **f** EDS analysis

Figure 3 displays the SEM images of B_2O_3 doped $CoNb_2O_6$ ceramics sintered at their respective optimum sintering temperatures. The microstructure of un-doped sample was also given here for comparison. After sintering at 1200 °C, pure $CoNb_2O_6$ ceramic exhibited dense microstructure with closely packed polygonal-shaped grains having 1–8 μm size (Fig. 3a). For the ceramic with 0.5 wt% B_2O_3 addition, some pores were still observed (see Fig. 3b). This might be a result of insufficient liquid phase. The number of pores appeared to decrease with the increase of B_2O_3 content. At a higher B_2O_3 content of 1.5 wt% in Fig. 3d, a fully-densified specimen was obtained with average grain size below 4 μm. On the whole, the average grain size of the B_2O_3-doped samples was found to be a little smaller than that of pure columbite. Thus, B_2O_3 doping, acting as a liquid phase, was believed to facilitate the densification of ceramics but inhibite the grain growth owing to a higher surface energy [20]. Nevertheless, further increasing B_2O_3 content induced considerable de-densification and exaggerated grain growth. From Fig. 3, it was easily to find that all specimens were composed of two kinds of polygon-like grains with different sizes, including the larger one (denoted as A), and the smaller one (denoted as B). Additionally, some elongated grains (denoted as C) existed in grain boundaries after the addition of 2 wt% B_2O_3, as seen in Fig. 3e. The composition of the different grains was qualitatively identified by EDS. The EDS analysis in Fig. 3f depicted that the polygonal-shaped grains were identified as $CoNb_2O_6$, and the elongated one was $Co_4Nb_2O_9$. It was also worth noting that no glass phase was found in Fig. 3, most likely due to the evaporation of B_2O_3 in the final stage.

The plot of ε_r is given in Fig. 4 as a function of sintering temperatures with various amounts of B_2O_3. As observed in Fig. 4, the ε_r values steadily increased first with increasing sintering temperature and then decreased after reaching the maximum values, exhibiting a similar trend to that of the relative densities. It was not difficult to accept since some of early researches had proved the influence of relative density on the dielectric properties. Higher density for samples meant there were more dipoles per unit volume, which indicated that the ceramics were more liable to be polarized. Hence, the improved densification could be responsible for the increase of ε_r in 0.5–1.5 wt% B_2O_3-doped samples. Nevertheless, the dielectric constants had a trend of decreasing at high B_2O_3-doping levels (2 wt%). This was ascribed to the comparatively lower permittivity

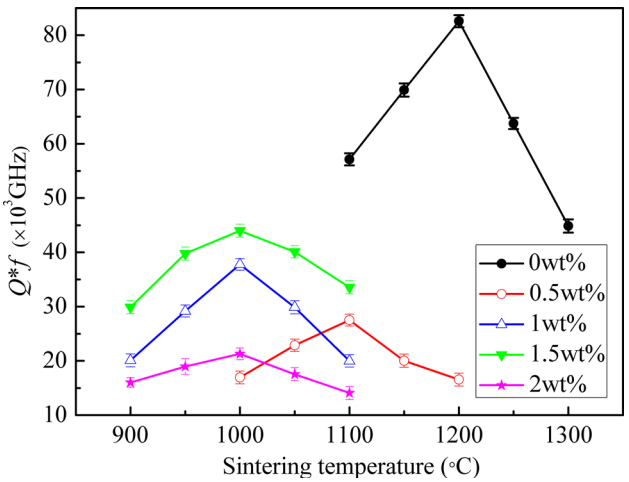

Fig. 5 Dependence of quality factors on sintering temperature for $CoNb_2O_6$ ceramics with various B_2O_3 additions

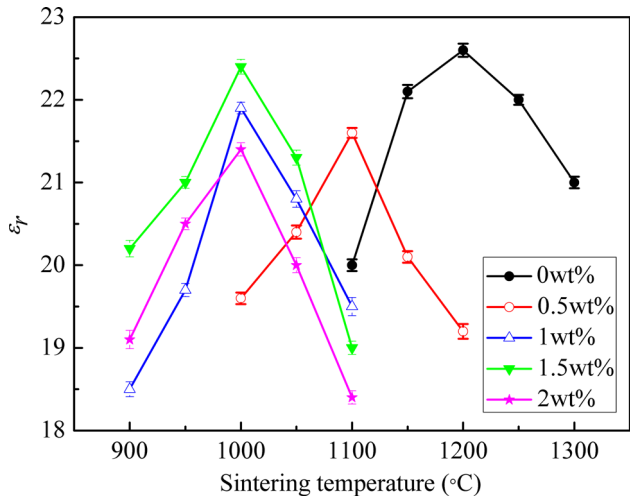

Fig. 4 Dielectric constants of B_2O_3-added $CoNb_2O_6$ ceramics as a function of sintering temperature

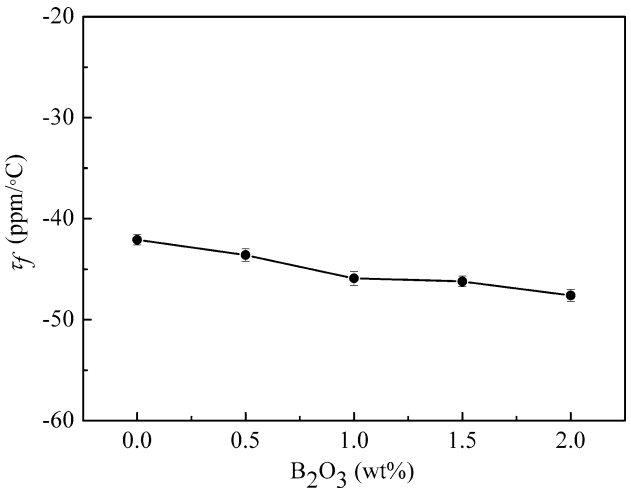

Fig. 6 Temperature coefficients of resonant frequency of $CoNb_2O_6$ ceramics as a function of B_2O_3 addition

Table 1 Sintering behavior and microwave dielectric properties of $CoNb_2O_6$ ceramics with B_2O_3 addition

$CoNb_2O_6$	*S.T.* (°C)	Relative density (%)	ε_r	$Q \times f$ (GHz)	τ_f (ppm/°C)
+0 wt% B_2O_3	1200	95.29	22.6	82,598	−42.1
+0.5 wt% B_2O_3	1100	95.57	21.6	27,505	−43.6
+1 wt% B_2O_3	1000	95.92	21.9	37,768	−45.9
+1.5 wt% B_2O_3	1000	96.72	22.4	43,979	−46.2
+2 wt% B_2O_3	1000	95.31	21.4	21,287	−47.6

S.T. sintering temperature

of the $Co_4Nb_2O_9$ (~16.0) compared to that of $CoNb_2O_6$ (~22.6) [19]. It was still possible that a slight amount of residual liquid phase could degrade the dielectric property.

Figure 5 illustrates the $Q \times f$ values of B_2O_3-added $CoNb_2O_6$ ceramics sintered at different temperatures for 4 h. Generally speaking, microwave dielectric loss included two parts: intrinsic loss and extrinsic loss. The intrinsic loss was mainly caused by lattice variation modes, while the extrinsic loss was dominated by densification, secondary phase, grains sizes, and lattice defects [21]. By increasing the sintering temperature, the $Q \times f$ of all compositions increased to the maximum values and declined thereafter. It was also found that the $Q \times f$ values of B_2O_3-doped samples were degraded even though the sintering behavior was greatly enhanced. This was because B_2O_3 doping restrained the grain growth, as seen in Fig. 3. The grain boundary was generally the site where dopants/impurities concentrated. As the average grain size became smaller, the total number of grain boundaries per unit volume increased, thereby resulting in higher dielectric loss [22]. With 0.5 wt% B_2O_3 additive, the $Q \times f$ of the ceramic sintered at 1100 °C was 27,505 GHz. This low value was due to the relatively inferior microstructure of the $CoNb_2O_6$ ceramic. The $Q \times f$ increased with increasing B_2O_3 concentration and got its maximum value of about 43,979 GHz at 1.5 wt% B_2O_3 addition, possibly depending on the removal of pores. However, further addition of B_2O_3 degraded the $Q \times f$ values drastically. This reduction was associated mostly with the presence of second phase $Co_4Nb_2O_9$ ($Q \times f \sim$ 5000 GHz) as well as the lattice defects produced in crystal growth [19]. In particular, a higher $Q \times f$ value (=82,598 GHz) of pure $CoNb_2O_6$ ceramic than that reported in Refs. [7–9] was obtained because of the additional screening process.

The τ_f values of $CoNb_2O_6$ ceramics with different B_2O_3 additions are depicted in Fig. 6. It is well known that τ_f largely depends on the composition, the amount of additives, and the second phases present in ceramics [23]. As listed in Fig. 6, the τ_f of un-doped $CoNb_2O_6$ ceramic exhibited a negative τ_f (~−42.1 ppm/°C). After the incorporation of B_2O_3, it shifted monotonically from −43.6 to −47.6 ppm/°C. This might result from the $Co_4Nb_2O_9$ s phase having a τ_f of −10 ppm/°C [19]. Moreover, increasing B_2O_3 amount probably led to an increase in the NbO_6 octahedral distortion, which would indirectly decline the τ_f to some extent. Specifically, the $CoNb_2O_6$ ceramic with 1.5 wt% B_2O_3 sintered at 1000 °C had the optimum dielectric values $\varepsilon_r = 22.4$, $Q \times f = 43{,}979$ GHz, and $\tau_f = -46.2$ ppm/°C, which outperformed the results achieved in [10].

The sintering behavior and microwave dielectric properties of B_2O_3-added $CoNb_2O_6$ ceramics sintered at their optimum temperatures are summarized in Table 1. There was no doubt that the sintering behavior in the present system was significantly enhanced by B_2O_3 doping. For 2 wt% B_2O_3-added $CoNb_2O_6$ ceramic, the sintering temperature was lowered to 1000 °C, accompanied by a substantially high $Q \times f$ of 43,979 GHz. The mentioned merits made it a very good potential for practical LTCC integration applications.

4 Conclusion

The effects of B_2O_3 addition on both the sintering behavior and microwave dielectric properties of $CoNb_2O_6$ ceramics had been investigated. The incorporation of B_2O_3 additives considerably decreased the sintering temperature to 1000 °C due to the liquid phase effect. A minor amount of hexagonal $Co_4Nb_2O_9$ was formed along with the major columbite phase at high B_2O_3 doping levels (2 wt%). Dielectric investigations shown that the addition of B_2O_3 to $CoNb_2O_6$ ceramics induced a limited degradation in ε_r and $Q \times f$. Typically, 1.5 wt% B_2O_3-doped $CoNb_2O_6$ ceramic exhibited a well-sintered microstructure with microwave dielectric properties of $\varepsilon_r = 22.4$, $Q \times f = 43{,}979$ GHz, and $\tau_f = -46.2$ ppm/°C at $T_s = 1000$ °C, making it a promising candidate for LTCC applications.

Acknowledgments This work has been sponsored by the National Natural Science Foundation of China (No. 51372017).

References

1. Y.C. Chen, Y.N. Wang, R.Y. Syu, J. Mater. Sci.: Mater. Electron. **27**, 4259 (2016)

2. A. Manan, D.N. Khan, A. Ullah, J. Mater. Sci.: Mater. Electron. **26**, 2066 (2015)
3. B. Tang, Z.X. Fang, H. Li, L. Liu, S.R. Zhang, J. Mater. Sci.: Mater. Electron. **26**, 300 (2015)
4. Y. Iqbal, R. Muhammad, J. Mater. Sci.: Mater. Electron. **27**, 1314 (2016)
5. K.A. Nekouee, R.A. Khosroshahi, R.T. Mousavian, N. Ehsani, J. Mater. Sci.: Mater. Electron. **27**, 3570 (2016)
6. N. Chaiyo, N. Vittayakorn, J. Ceram. Process. Res. **9**, 381 (2008)
7. H.J. Lee, K.S. Hong, S.J. Kim, Mater. Res. Bull. **32**, 847 (1997)
8. R.C. Pullar, J.D. Breeze, N.M. Alford, J. Am. Ceram. Soc. **88**, 2466 (2005)
9. A.G. Belous, O.V. Ovchar, A.V. Kramarenko, D.O. Mishchuk, B. Jancar, J. Bezjak, D. Suvorov, Inorg. Mater. **42**, 1369 (2006)
10. R.C. Pullar, C. Vaughan, N.M. Alford, J. Phys. D Appl. Phys. **37**, 348 (2004)
11. J.S. Kim, M.E. Song, M.R. Joung, J.H. Choi, S. Nahm, S. Gu, J.H. Paik, B.H. Choi, J. Eur. Ceram. Soc. **30**, 375 (2010)
12. Y. Lv, R.Z. Zuo, Ceram. Int. **39**, 2545 (2013)
13. B.W. Hakki, P.D. Coleman, IEEE Trans. Microw. Theory Tech. **8**, 402 (1960)
14. W.E. Courtney, IEEE Trans. Microw. Theory Tech. **18**, 476 (1970)
15. Y. Kobayashiy, M. Katoh, IEEE Trans. Microw. Theory Tech. **33**, 586 (1985)
16. H.T. Wu, Q.J. Mei, J. Alloys Compd. **651**, 393 (2015)
17. L.C. Chang, B.S. Chiou, J. Electroceram. **13**, 829 (2004)
18. M.K. Ekmekçi, M. Erdem, A.S. Başak, Dalton Trans. **44**, 5379 (2015)
19. A. Kan, H. Ogawa, A. Yokoi, Y. Nakamura, J. Eur. Ceram. Soc. **27**, 2977 (2007)
20. J.M. Li, B. Yao, D.C. Xu, Z.X. Huang, Z.J. Wang, X. Wu, C.G. Fan, J. Alloys Compd. **663**, 494 (2016)
21. D. Zhou, C.A. Randall, L.X. Pang, H. Wang, J. Guo, G.Q. Zhang, X.G. Wu, L. Shui, X. Yao, J. Am. Ceram. Soc. **94**, 348 (2011)
22. Y. Zhang, Y.C. Zhang, B.J. Fu, M. Hong, M.Q. Xiang, Ceram. Int. **41**, 10243 (2015)
23. Y.C. Chen, Y.W. Zeng, J. Alloys Compd. **481**, 369 (2009)